Mechanochromic luminescence and solid-state circularly polarized luminescence of a chiral diamine-linked bispyrene

Suguru Ito,*[a] Ryohei Sekine,[a] Masayasu Munakata,[a] Masatoshi Asami,[a] Takashi Tachikawa,[b,c] Daiki Kaji,[d] Kohei Mishima,[d] and Yoshitane Imai*[d]

[a] Prof. Dr. S. Ito, R. Sekine, M. Munakata, Prof. Dr. M. Asami
Department of Chemistry and Life Science, Graduate School of Engineering Science
Yokohama National University
79-5, Tokiwadai, Hodogaya-ku, Yokohama 240-8501 (Japan)
E-mail: suguru-ito@ynu.ac.jp
[b] Prof. Dr. T. Tachikawa
Department of Chemistry, Graduate School of Science
Kobe University
1-1 Rokkodai-cho, Nada-ku, Kobe 657-8501 (Japan)
[c] Prof. Dr. T. Tachikawa
Molecular Photoscience Research Center, Kobe University
1-1 Rokkodai-cho, Nada-ku, Kobe 657-8501 (Japan)
[d] D. Kaji, K. Mishima, Prof. Dr. Y. Imai
Department of Applied Chemistry, Faculty of Science and Engineering
Kindai University
3-4-1 Kowakae, Higashi-Osaka, Osaka 577-8502 (Japan)
E-mail: y-imai@apch.kindai.ac.jp

Supporting information for this article is given via a link at the end of the document.

Abstract: Despite the recent increased interest in organic small molecule luminophores that exhibit circularly polarized luminescence (CPL) or mechanochromic luminescence (MCL), MCL behavior in chiral luminophores that display solid-state CPL still remains elusive. Herein, it is reported that a chiral diamine-linked bispyrene **1** exhibits a rare MCL behavior in response to two different types of mechanical stimuli: Ultrasonication and grinding. Moreover, an unprecedented switching of solid-state CPL has been achieved for the chiral **1** between two states that can respond to the different mechanical stimuli. These findings should help to advance the development of practical CPL materials.

Introduction

Circularly polarized luminescence (CPL) describes the differential emission of left- or right-handed circularly polarized light from chiral luminophores.[1] Chiral organic molecules that exhibit CPL have recently attracted considerable attention owing to their unique advantages, such as the tunability of their emission properties and their processability for the manufacturing of composite materials.[1c–e] Moreover, the phenomenon of CPL switching in response to an external stimulus,[1d,2–7] such as ions,[2] light,[3] pH,[4] solvents,[2d,5] temperature,[6] and chemicals,[7] has been a particular focus. Such CPL-switching materials can potentially find applications in 3D-switching devices, anti-counterfeiting technologies, cryptographic communication, and sensing devices. However, most typical CPL-switching systems have been evaluated in solution (Figure 1a). Since only a limited number of solid-state-emissive CPL materials has been reported to date,[8] little is known about the CPL switching in solid materials, especially in the case of small chiral organic molecules.[9]

Mechanical stimuli are a common class of external stimuli that can induce the switching of physical properties in solid materials. The term mechanochromic luminescence (MCL) refers to a reversible mechanical-stimuli-induced change of the emission color of solid luminophores, and has recently been investigated intensively due to numerous promising applications of MCL materials in e.g. mechanosensors and security technologies.[10] In typical organic MCL molecules, the emission color can be switched by grinding a powdered sample, and the original color can be recovered via heating or exposure to solvents (Figure 1b). The MCL of most crystalline organic molecules has been attributed to phase transitions between crystalline and amorphous phases.[11] During the recent development of advanced organic MCL molecules, several chiral organic luminophores have been reported to exhibit MCL.[12] However, only a few exhibit mechano-responsive switching of the solid-state CPL, whereby the original state is recovered from the mechanically induced state by heating or solvent fuming.[9b] Further investigations are thus required to develop chiral luminophores that exhibit versatile MCL switching of their solid-state CPL, as such luminophores could expand the potential applications of both MCL and CPL materials.

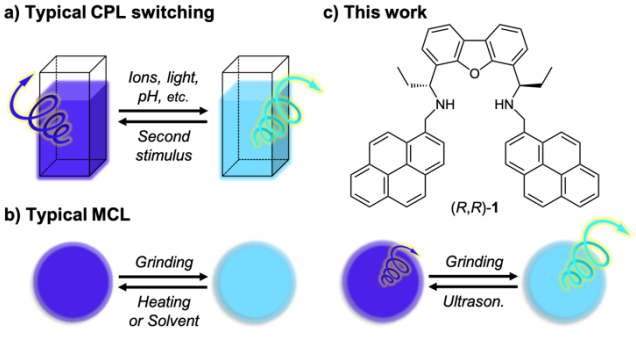

Figure 1. a) Typical CPL switching: Solution-state switching in response to external stimuli. b) Typical MCL: Switching by mechanical stimuli such as grinding and by heating or solvent exposure. c) This work: CPL switching between two states that can respond to two different mechanical stimuli.

Several pyrene-based compounds show the CPL switching in solution state.[1c,3d,e,5c] We have recently reported the solution-state CPL switching of a dibenzofuran-based C_2-symmetric *N*,*N*′-dipyrenyldiamine between the monomer and excimer emission regions of the pyrene groups under the inversion of the CPL handedness.[13] Herein, we report the rare MCL behavior of the dibenzofuran-based C_2-symmetric *N*,*N*′-bis(pyrenylmethyl)diamine (*R*,*R*)-**1**, whose solid-state emission color can be switched between two states in response to ultrasonication and grinding (Figure 1c). Remarkably, the two states exhibit different solid-state CPL properties. To the best of our knowledge, this is the first example of solid-state CPL switching of an organic compound between two states that can respond to two different mechanical stimuli.[11c, 14]

Results and Discussion

Chiral secondary diamine (*R*,*R*)-**1** was synthesized according to our literature procedure (Scheme S1):[15] A diimine precursor for (*R*,*R*)-**1**, prepared from the corresponding primary diamine and pyrene-1-carbaldehyde, was treated with sodium cyanoborohydride. The resulting crude product was purified using column chromatography on silica gel, followed by evaporation of the solvent (CH_2Cl_2/hexane) under reduced pressure to afford the as-prepared powdered sample of (*R*,*R*)-**1**. Under UV irradiation (λ_{ex} = 365 nm), as-prepared (*R*,*R*)-**1** exhibited intense blue-green emission. The maximum emission wavelength (λ_{em}) and emission quantum yield (Φ_F) of the blue-green emission were 484 nm and 0.46, respectively (Figure 2). A powder X-ray diffraction (PXRD) analysis of as-prepared (*R*,*R*)-**1** showed no diffraction peaks (Figure 3a). Therefore, the blue-green-emissive powder of (*R*,*R*)-**1** is in an amorphous state (abbreviated henceforth as **1A**).

Sonocrystallization is a well-known technique to induce crystallization from amorphous samples.[16] In order to induce crystallization, a suspension of (*R*,*R*)-**1A** in hexane was exposed to ultrasound (40 kHz).[17] The solid sample collected by filtration of the ultrasonicated suspension exhibited a relatively weak violet emission (λ_{em} = 413 nm, Φ_F = 0.06; Figure 2). This solid exhibited intense PXRD peaks, indicating that a phase transition from an amorphous (*R*,*R*)-**1A** to a crystalline state (henceforth denoted as **1C**) occurred upon ultrasonication (Figure 3b). Scanning electron microscopy (SEM) measurements showed a sheet-like structure for (*R*,*R*)-**1A** and aggregates of a fine powder for (*R*,*R*)-**1C** (Figure 4a and b). Remarkably, the microsheets of (*R*,*R*)-**1A** acted as optical waveguides.[18] In single-particle-level observations using fluorescence microscopy, intense emission was only observed at the edges of the microsheets (Figure 4d inset and Figure S1).[19] In contrast, the entire aggregates of (*R*,*R*)-**1c** exhibited luminescence (Figure 4c inset).

Although a single crystal suitable for X-ray diffraction analysis could not be obtained for (*R*,*R*)-**1C** from various solvents, the violet emission from (*R*,*R*)-**1C** was attributed to monomer emission from the pyrenyl group based on the wavelength and vibrational structures of the emission band (Figure 2). In addition, (*R*,*R*)-**1C** exhibited a mean fluorescence lifetime (<τ>) of 3.6 ns (Figures 4c, S2 and Table S1). The fluorescence lifetime for the monomer emission of pyrenyl groups in the crystalline state is often less than 10 ns,[20] which

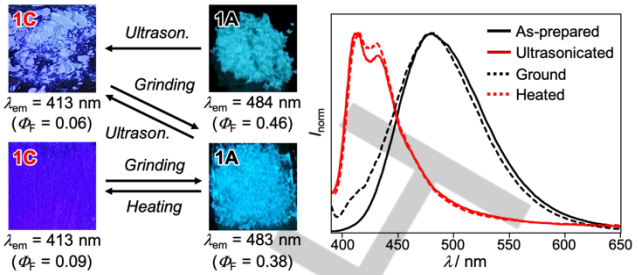

Figure 2. Photographs and normalized fluorescence spectra of the MCL of (*R*,*R*)-**1** (λ_{ex} = 365 nm).

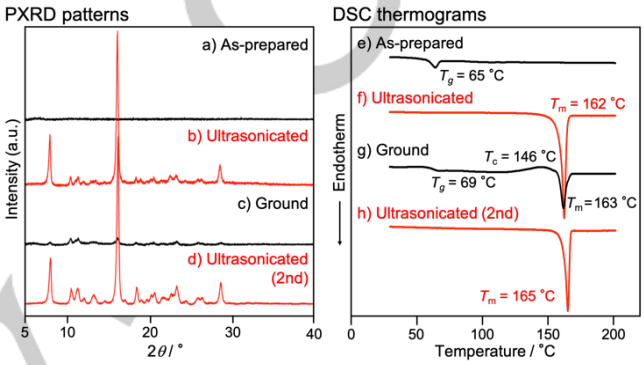

Figure 3. PXRD patterns and DSC thermograms of (*R*,*R*)-**1**. a and e) As-prepared samples after evaporation of the solvent. b and f) After ultrasonication of the as-prepared samples. c and g) After grinding of the ultrasonicated samples. d and h) After ultrasonication of the ground samples. T_g, T_m, and T_c values are noted near the corresponding peaks and steps.

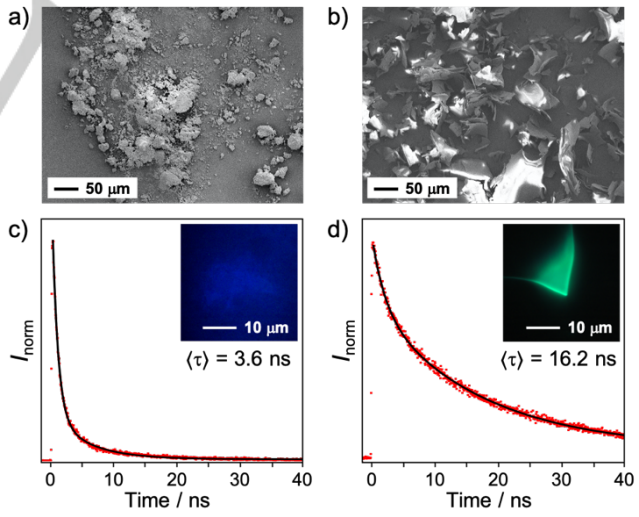

Figure 4. SEM images of a) ultrasonicated (*R*,*R*)-**1C** and b) as-prepared (*R*,*R*)-**1A**. Fluorescence decay profiles and photographs (inset) of c) ultrasonicated (*R*,*R*)-**1C** and d) as-prepared (*R*,*R*)-**1A** recorded at the single-particle level (λ_{ex} = 405 nm).

stands in sharp contrast to the long fluorescence lifetime (>100 ns) of the monomer emission from pyrene in solution. On the other hand, the emission band of (*R*,*R*)-**1A** was assigned to the excimer emission from intra- or intermolecularly stacked pyrenyl

groups. The decay curve of (*R*,*R*)-**1A** indicated a <τ> value of 16.2 ns (Figure 4d and Table S1), which is in good agreement with the reported fluorescence lifetime of pyrene excimers in the crystalline state.[21]

The excimer emission from (*R*,*R*)-**1A** was attributed to the formation of dynamic excimers[22] in the excited state. The absorption spectra of (*R*,*R*)-**1A** and (*R*,*R*)-**1C** (Figure S3) were observed in almost the same region. Moreover, the excitation spectrum of (*R*,*R*)-**1A** (λ_{em} = 483 nm) was in good agreement with that of (*R*,*R*)-**1C** (λ_{em} = 413 nm) (Figure S4). These results suggest that the pyrenyl groups did not form dimeric structures in the ground state. It should also be noted here that the immediate formation of the excimers from the monomer pyrenyl groups on the picosecond time scale[23] should account for the absence of a rise component in the decay profile of (*R*,*R*)-**1A**.

Upon grinding (*R*,*R*)-**1C** using a spatula, an intense blue-green emission (λ_{em} = 483 nm, Φ_F = 0.38) was observed, similar to that of as-prepared (*R*,*R*)-**1A** (Figure 2). The amorphization of the crystal structure upon grinding was confirmed by a PXRD analysis of the ground sample (Figure 3c). Subsequent ultrasonication of ground (*R*,*R*)-**1A** restored its weak violet emission (λ_{em} = 413 nm) and intense PXRD patterns (Figure 3d). In other words, (*R*,*R*)-**1** exhibits MCL that responds to two types of mechanical stimuli, i.e., ultrasonication and grinding. The MCL conversion between (*R*,*R*)-**1A** and (*R*,*R*)-**1C** could be repeated for at least five cycles (Figure 5). The maximum emission wavelengths of amorphous and crystalline (*R*,*R*)-**1** were observed within experimental errors during the fifth ultrasonication–grinding cycles between **1A** and **1C**, supporting the absence of decomposition of (*R*,*R*)-**1**. The transition from the amorphous to the crystalline state and the accompanying emission-color change were also achieved upon heating ground (*R*,*R*)-**1A** to 150 °C (Figures 2 and S5). However, as-prepared (*R*,*R*)-**1A** could not be transformed into (*R*,*R*)-**1C** by heating. These results suggest that residual traces of crystalline phases in ground (*R*,*R*)-**1A** are necessary to facilitate the recrystallization of (*R*,*R*)-**1C** upon heating.

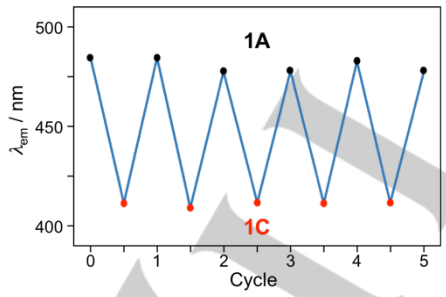

Figure 5. Plots of the emission maxima during the fifth ultrasonication–grinding cycles.

The occurrence of crystal-to-amorphous phase transitions in the MCL of (*R*,*R*)-**1** was also supported by an analysis of the thermo-induced phase transitions of (*R*,*R*)-**1** using differential scanning calorimetry (DSC). In the DSC thermogram of as-prepared (*R*,*R*)-**1A**, a glass-transition temperature (T_g) was observed at 65 °C together with an enthalpy-relaxation peak (Figure 3e). Ultrasonicated (*R*,*R*)-**1C** showed an endothermic melting point (T_m) at 162 °C (Figure 3f). These results indicate that as-prepared (*R*,*R*)-**1A** and ultrasonicated (*R*,*R*)-**1C** exist in the amorphous and crystalline states, respectively. The DSC measurements confirmed that ground (*R*,*R*)-**1A** crystallizes upon heating, whereas crystallization does not occur when heating as-prepared (*R*,*R*)-**1A**. Specifically, ground (*R*,*R*)-**1A** showed a T_g at 69 °C, followed by a cold-crystallization transition peak (T_c) at 146 °C and T_m at 163 °C (Figure 3g). The cold crystallization of ground (*R*,*R*)-**1A** should be attributed to the facilitation of recrystallization by the residual traces of crystalline phases. Crystalline (*R*,*R*)-**1C**, obtained from the ultrasonication of ground (*R*,*R*)-**1A**, exhibited only one endothermic peak (T_m = 165 °C; Figure 3h).

We also carried out CPL measurements of crystalline (*R*,*R*)-**1C** and amorphous (*R*,*R*)-**1A**. Reflecting the fact that the emission of (*R*,*R*)-**1** was switched between monomer and excimer emission, the CPL characteristics were also switched for (*R*,*R*)-**1C** and **1A**. A negative CPL band was detected in the excimer emission region for (*R*,*R*)-**1A** (Figure 6b). In contrast, for crystalline (*R*,*R*)-**1C**, the CPL band was not observed in the excimer emission region, and negative CPL signals were observed in the monomer emission region (Figure 6a). Since the Φ_F value of **1C** is considerably smaller than that of **1A** (**1C**: Φ_F = 0.06; **1A**: Φ_F = 0.46), the CPL intensity of **1C** was significantly weaker than that of **1A**.[24] We also synthesized the enantiomer (*S*,*S*)-**1**, which shows identical MCL behavior (Scheme S2 and Figure S6). Both (*S*,*S*)-**1C** and (*S*,*S*)-**1A** exhibit positive CPL signals in the same regions as (*R*,*R*)-**1C** and (*R*,*R*)-**1A**, respectively (Figure 6). These results exclude the possibility of any artifacts in the CPL switching in response to mechanical stimuli.[25] The absolute value of Kuhn's dimensionless anisotropy factor (|g_{CPL}|) is defined as $g_{CPL} = 2(I_L - I_R)/(I_L + I_R)$.[26] The averaged g_{CPL} value for the enantiomeric CPL bands of **1A** is 2.0 × 10^{-3} (λ_{CPL} = 490 nm), which is smaller than the excimer g_{CPL} value of **1** in toluene (g_{CPL} = 1.1 × 10^{-2}).[27] Although the exact reason is unclear at this moment, the restriction of molecular motion and formation of intermolecular stacks in the solid state would account for the relatively small g_{CPL} value of **1A** compared to that in the solution state.[28]

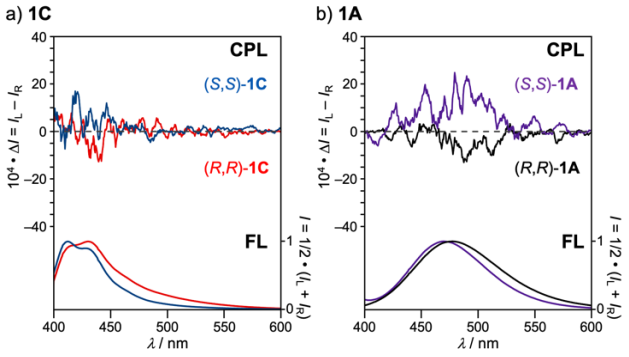

Figure 6. Normalized CPL (top) and fluorescence (FL, bottom) spectra of a) **1C** and b) **1A** for (*R*,*R*)- (red and black) and (*S*,*S*)- (blue and violet) samples.

Conclusion

In summary, the different solid-state CPL properties of chiral *N*,*N*′-bis(pyrenylmethyl)diamine **1** can be observed between two states that can respond to mechanical stimuli. The intense

excimer emission from **1A** was switched to the relatively weak monomer emission from **1C** upon ultrasonication. Ultrasonication-induced crystallization of as-prepared amorphous solids can thus be considered as an effective method to obtain MCL crystals with different CPL properties. It was possible to revert ground amorphous samples of **1** to the crystalline state using ultrasonication and heating. The mechanism of the MCL should be attributed to the switching between monomer and excimer emission due to the crystal-to-amorphous transitions. Moreover, as-prepared amorphous **1** exhibited optical waveguide behavior, which is unprecedented for CPL-active organic molecules, that may lead to applications in CPL waveguides. As the area of mechano-responsive solid-state CPL switching is still in its infancy, the basic insights obtained in this study can be expected to promote future developments of new chiral MCL materials.

Experimental Section

General

All air-sensitive experiments were carried out under an argon atmosphere unless otherwise noted. Silica gel 60 N (spherical, neutral, 63–210 μm) was used for column chromatography. (*R*,*R*)-4,6-Bis(1-aminopropyl)dibenzo[*b*,*d*]furan (**S1**) and (*S*,*S*)-**S1** (Scheme S1 and S2) were synthesized by our previously reported procedure.[15a] Other reagents and solvents were commercially available and were used as received. ^{1}H and ^{13}C NMR spectra were recorded on a JEOL ECA500 spectrometer using tetramethylsilane as an internal standard. High-resolution mass spectra (HRMS-ESI) were recorded on a Hitachi Nano Frontier LD spectrometer. Optical rotation was measured on a JASCO P-1000 automatic polarimeter. A miniature fiber-optic spectrometer (FLAME-S-XR1-ES, Ocean Optics) and a handy UV lamp (365 nm, LUV-6, AS ONE) were used for the measurements of mechanochromic luminescence (MCL). Fluorescence spectra were measured on a JASCO FP-8300 fluorescence spectrometer. The solid-state absorption spectra were obtained by measuring diffuse reflectance spectra using an FPA-810 powder sample cell block. The absolute fluorescence quantum yields were determined using a 100 mm ϕ integrating sphere JASCO ILF-835. Powder X-ray diffraction (PXRD) measurements were performed on a Rigaku SmartLab system using CuKα radiation. Differential scanning calorimetry (DSC) data were recorded on a Shimadzu DSC-60 plus (heating rate: 10 °C min^{-1}). The SEM images were taken using a Keyence VE8800. The ultrasonic irradiation was applied by using a MUJIGAE SD-120H with the nominal frequency of 40 kHz.

Synthesis of (*R*,*R*)-1A

In accordance with the previously reported procedure,[15a] chiral diamine (*R*,*R*)-**1** was synthesized from (*R*,*R*)-4,6-bis(1-aminopropyl)dibenzo[*b*,*d*]furan (**S1**) and pyrene-1-carbaldehyde (Scheme S1). The crude product of (*R*,*R*)-**1** was purified by column chromatography on silica gel twice (Silica gel 60N; first with hexane/CH_2Cl_2/AcOEt = 1:2:1 and then with CH_2Cl_2). The purified product was dissolved in CH_2Cl_2/hexane, and the solvents were evaporated under reduced pressure to give (*R*,*R*)-**1A** as a white solid.

(*R*,*R*)-4,6-Bis{1-[(pyren-1-ylmethyl)amino]propyl}dibenzo[*b*,*d*]furan (1) White solid; T_g 64.7 °C; $[\alpha]_D^{26}$ +12.8 (*c* 1.0, $CHCl_3$); ^{1}H NMR (500 MHz, $CDCl_3$): δ (ppm) 7.99–7.75 (m, 18H), 7.67 (d, *J* = 7.6 Hz, 2H), 7.57 (d, *J* = 7.6 Hz, 2H), 7.46 (t, *J* = 7.6 Hz, 2H), 4.21 (dd, *J* = 7.6, 6.2 Hz, 2H), 4.14 (d, *J* = 12.3 Hz, 2H), 4.03 (d, *J* = 12.3 Hz, 2H), 1.99–1.85 (m, 6H), 0.81 (t, *J* = 7.3 Hz, 6H); ^{13}C NMR (126 MHz, $CDCl_3$): δ (ppm) 154.4, 133.9, 131.1, 130.7, 130.5, 129.0, 128.3, 127.3, 127.2, 127.1, 126.8, 126.1, 125.6, 124.82, 124.76, 124.70, 124.5, 124.4, 123.14, 123.06, 119.2, 60.6, 49.9, 29.8, 11.1 (one signal is hidden due to the incidental overlapping); HRMS (*m*/*z*): [M+H]$^+$ Calcd for $C_{52}H_{43}N_2O$, 711.3375; Found, 711.3372. ^{1}H and ^{13}C NMR spectra of (*R*,*R*)-**1A** were in good agreement with those of previously reported (*R*,*R*)-**1**.[15a]

Synthesis of (*S*,*S*)-1A

In accordance with the same experimental procedure as the synthesis of (*R*,*R*)-**1**, chiral diamine (*S*,*S*)-**1** was synthesized by the reaction of (*S*,*S*)-**S1** (0.10 g, 0.37 mmol) and pyrene-1-carbaldehyde (187 mg, 0.81 mmol) in MeOH (9 mL) followed by treating with $NaBH_3CN$ (70 mg, 1.1 mmol) (Scheme S2). The crude product was purified by the same procedure as that for (*R*,*R*)-**1A**, and as-prepared (*S*,*S*)-**1A** (97 mg, 40%) was obtained as a white solid.

(*S*,*S*)-4,6-Bis{1-[(pyren-1-ylmethyl)amino]propyl}dibenzo[*b*,*d*]furan (1) White solid; $[\alpha]_D^{25}$ –13.5 (*c* 1.0, $CHCl_3$); ^{1}H NMR (500 MHz, $CDCl_3$): δ (ppm) 8.01–7.76 (m, 18H), 7.69 (d, *J* = 7.6 Hz, 2H), 7.58 (d, *J* = 7.6 Hz, 2H), 7.47 (t, *J* = 7.6 Hz, 2H), 4.22 (dd, *J* = 7.6, 6.2 Hz, 2H), 4.16 (d, *J* = 12.3 Hz, 2H), 4.04 (d, *J* = 12.3 Hz, 2H), 1.99–1.82 (m, 6H), 0.82 (t, *J* = 7.3 Hz, 6H); ^{13}C NMR (126 MHz, $CDCl_3$): δ (ppm) 154.4, 133.9, 131.1, 130.7, 130.5, 129.0, 128.3, 127.3, 127.23, 127.15, 126.8, 126.1, 125.6, 124.84, 124.77, 124.72, 124.5, 124.4, 123.2, 123.1, 119.2, 60.6, 49.9, 29.8, 11.1 (one signal is hidden due to the incidental overlapping); HRMS-ESI (*m*/*z*): [M+H]$^+$ Calcd for $C_{52}H_{43}N_2O$, 711.3375; Found, 711.3385.

Experimental procedure for the MCL of (*R*,*R*)-1

A suspension of as-prepared (*R*,*R*)-**1A** (30 mg) in hexane (5.0 mL) was ultrasonicated for 60 s in an ultrasonic bath at a frequency of 40 kHz. The resulting white precipitates of (*R*,*R*)-**1C** were collected by vacuum filtration using a membrane filter (22.5 mg, 75% recovery). Several pieces of (*R*,*R*)-**1C**, placed on a glass plate, were ground manually with a spatula to afford (*R*,*R*)-**1A**. The ground (*R*,*R*)-**1A** was recovered to (*R*,*R*)-**1C** by ultrasonication in hexane or heating on a hot plate to 150 °C.

Single-particle level observations and the measurement of fluorescence lifetimes

Single-particle fluorescence measurements were performed on a home-built wide-field/confocal microscope equipped with a Nikon Ti-E inverted fluorescence microscope. The fluorescence images were recorded using a color sCMOS camera (Dhyana 400DC, Tucsen Photonics). The 405-nm continuous wave laser (OBIS 405LX, Coherent) or 405-nm pulsed diode laser (PiL040X, Advanced Laser Diode System, 45-ps FWHM) was used to excite the samples. A dichroic mirror (Di02-R405, Semrock) and a longpass filter (ET425lp, Chroma) were used to filter the scattering from excitation light. For the spectroscopy, only the emission that passed through a slit entered the imaging spectrograph (MS3504i, SOL instruments) equipped with a CCD camera (DU416A-LDC-DD, Andor). For time-resolved fluorescence measurements, the emitted photons were passed through a 100-μm pinhole and then directed onto a single-photon avalanche diode (SPD-050, Micro Photon Devices). The signals from the detector were sent to a time-correlated single photon counting module (SPC-130EM, Becker & Hickl) for further analysis. The instrument response function of the system was about 100 ps. All the experiments were conducted at room temperature. The data were analyzed using ImageJ (http://rsb.info.nih.gov/ij/) and Origin 2021 (OriginLab).

Measurement of CPL and FL spectra of enantiomeric 1C and 1A

The FL and CPL spectra of the luminophores were measured using the JASCO CPL-300 spectrofluoropolarimeter[29] at room temperature at a scattering angle of 0° upon excitation with an unpolarized, monochromatic incident light with a 10-nm bandwidth. The excitation wavelength for all samples was 365 nm. Scanning speed, cumulative

number, and response were set at 50 nm/min, 2 times, and 8 sec, respectively. A 0.1-mm path length was used for the solid-state spectroscopic measurements. Powdered samples were placed on a 0.1-mm quartz cell with an area of 10 mm in length and width.

Acknowledgements

This work was partly supported by JSPS KAKENHI Grant Numbers 18K05094 and 20K05645 within the Grant-in-Aid for Scientific Research (C), JSPS KAKENHI Grant Numbers 18H04508, 20H04665, 20H04673, and 20H04678 within the Grant-in-Aid for Scientific Research on Innovative Areas “Soft Crystals: Area No. 2903”, and JST CREST Grant Number JPMJCR2001, Japan. The part of this work was carried out by the joint research program No. R02019 of Molecular Photoscience Research Center, Kobe University.

Keywords: dyes/pigments • luminescence • mechanochromism • photochemistry

[1] For recent reviews, see: a) Y. Kitagawa, M. Tsurui, Y. Hasegawa, *ACS Omega* **2020**, *5*, 3786; b) Y. Sang, J. Han, T. Zhao, P. Duan, M. Liu, *Adv. Mater.* **2020**, *32*, 1900110; c) Y. Ohishi, M. Inouye, *Tetrahedron Lett.* **2019**, *60*, 151232; d) J.-L. Ma, Q. Peng, C.-H. Zhao, *Chem. - Eur. J.* **2019**, *25*, 15441; e) W.-L. Zhao, M. Li, H.-Y. Lu, C.-F. Chen, *Chem. Commun.* **2019**, *55*, 13793; f) J. Han, S. Guo, H. Lu, S. Liu, Q. Zhao, W. Huang, *Adv. Opt. Mater.* **2018**, *6*, 1800538.

[2] For recent examples of ion-responsive CPL switching, see: a) Y. Mimura, T. Sato, Y. Motomura, H. Yoshikawa, M. Shizuma, M. Kitamatsu, Y. Imai, *RSC Adv.* **2020**, *10*, 2575; b) E. Lee, Y. Hosoi, H. Temma, H. Ju, M. Ikeda, S. Kuwahara, Y. Habata, *Chem. Commun.* **2020**, *56*, 3373; c) Z.-B. Sun, J.-K. Liu, D.-F. Yuan, Z.-H. Zhao, X.-Z. Zhu, D.-H. Liu, Q. Peng, C.-H. Zhao, *Angew. Chem. Int. Ed.* **2019**, *58*, 4840; d) Y. Imai, J. Yuasa, *Chem. Commun.* **2019**, *55*, 4095; e) D. Niu, Y. Jiang, L. Ji, G. Ouyang, M. Liu, *Angew. Chem. Int. Ed.* **2019**, *58*, 5946. f) S. P. Morcillo, D. Miguel, L. Álvarez de Cienfuegos, J. Justicia, S. Abbate, E. Castiglioni, C. Bour, M. Ribagorda, D. J. Cárdenas, J. M. Paredes, L. Crovetto, D. Choquesillo-Lazarte, A. J. Mota, M. C. Carreño, G. Longhi, J. M. Cuerva, *Chem. Sci.* **2016**, *7*, 5663; g) H. Isla, M. Srebro-Hooper, M. Jean, N. Vanthuyne, T. Roisnel, J. L. Lunkley, G. Muller, J. A. Gareth Williams, J. Autschbach, J. Crassous, *Chem. Commun.* **2016**, *52*, 5932; h) H. Maeda, Y. Bando, K. Shimomura, I. Yamada, M. Naito, K. Nobusawa, H. Tsumatori, T. Kawai, *J. Am. Chem. Soc.* **2011**, *133*, 9266.

[3] For examples of photo-responsive CPL switching, see: a) H. Jiang, Y. Jiang, J. Han, L. Zhang, M. Liu, *Angew. Chem. Int. Ed.* **2019**, *58*, 785; b) Y. Wang, Y. Jiang, X. Zhu, M. Liu, *J. Phys. Chem. Lett.* **2019**, *10*, 5861; c) L. Ji, Q. He, D. Niu, J. Tan, G. Ouyang, M. Liu, *Chem. Commun.* **2019**, *55*, 11747; d) A. Homberg, E. Brun, F. Zinna, S. Pascal, M. Górecki, L. Monnier, C. Besnard, G. Pescitelli, L. D. Bari, J. Lacour, *Chem. Sci.* **2018**, *9*, 7043; e) Y. Hashimoto, T. Nakashima, D. Shimizu, T. Kawai, *Chem. Commun.* **2016**, *52*, 5171.

[4] For examples of pH-responsive CPL switching, see: a) D. Niu, L. Ji, G. Ouyang, M. Liu, *ACS Appl. Mater. Interfaces* **2020**, *12*, 18148; b) H. Yu, B. Zhao, J. Guo, K. Pan, J. Deng, *J. Mater. Chem. C* **2020**, *8*, 1459; c) A. H. G. David, R. Casares, J. M. Cuerva, A. G. Campaña, V. Blanco, *J. Am. Chem. Soc.* **2019**, *141*, 18064; d) T. Otani, A. Tsuyuki, T. Iwachi, S. Someya, K. Tateno, H. Kawai, T. Saito, K. S. Kanyiva, T. Shibata, *Angew. Chem. Int. Ed.* **2017**, *56*, 3906; e) S. Pascal, C. Besnard, F. Zinna,L.D.Rari, B. Le Guennic, D. Jacquemin, J. Lacour, *Org. Biomol. Chem.* **2016**, *14*, 4590.

[5] For examples of solvent-dependent CPL switching, see: a) K. Takaishi, K. Iwachido, T. Ema, *J. Am. Chem. Soc.* **2020**, *142*, 1774; b) M.-M. Zhang, X.-Y. Dong, Z.-Y. Wang, H.-Y. Li, S.-J. Li, X. Zhao, S.-Q. Zang, *Angew. Chem. Int. Ed.* **2020**, *59*, 10052; c) H. Anetai, T. Takeda, N. Hoshino, Y. Araki, T. Wada, S. Yamamoto, M. Mitsuishi, H. Tsuchida, T. Ogoshi, T. Akutagawa, *J. Phys. Chem. C* **2018**, *122*, 6323.

[6] For examples of thermo-responsive CPL switching, see: a) K. Hirano, T. Ikeda, N. Fujii, T. Hirao, M. Nakamura, Y. Adachi, J. Ohshita, T. Haino, *Chem. Commun.* **2019**, *55*, 10607; b) J. Chen, Y. Chen, L. Zhao, L. Feng, F. Xing, C. Zhao, L. Hu, J. Ren, X. Qu, *J. Mater. Chem. C* **2019**, *7*, 13947.

[7] For examples of CPL sensing for chiral compounds, see: a) M. Iwamura, M. Fujii, A. Yamada, H. Koike, K. Nozaki, *Chem. - Asian J.* **2019**, *14*, 561; b) T. Zhao, J. Han, X. Jin, Y. Liu, M. Liu, P. Duan, *Angew. Chem. Int. Ed.* **2019**, *58*, 4978; c) D. Wu, Z. Zhang, X. Chen, L. Meng, C. Li, G. Li, X. Chen, Z. Shi, S. Feng, *Chem. Commun.* **2019**, *55*, 14918.

[8] For examples of solid-state CPL, see: a) C.-L. Sun, J. Li, Q.-W. Song, Y. Ma, Z.-Q. Zhang, J.-B. De, Q. Liao, H. Fu, J. Yao, H.-L. Zhang, *Angew. Chem. Int. Ed.* **2020**, *59*, 11080; b) K. Takaishi, R. Takehana, T. Ema, *Chem. Commun.* **2018**, *54*, 1449; c) K. Takaishi, T. Yamamoto, S. Hinoide, T. Ema, *Chem. - Eur. J.* **2017**, *23*, 9249; d) H. Nishimura, K. Tanaka, Y. Morisaki, Y. Chujo, A. Wakamiya, Y. Murata, *J. Org. Chem.* **2017**, *82*, 5242; e) J. Kumar, T. Nakashima, H. Tsumatori, T. Kawai, *J. Phys. Chem. Lett.* **2014**, *5*, 316; f) J. C. Y. Ng, J. Liu, H. Su, Y. Hong, H. Li, J. W. Y. Lam, K. S. Wong, B. Z. Tang, *J. Mater. Chem. C* **2014**, *2*, 78.

[9] Very few organic molecules exhibit solid-state CPL switching; for details, see: a) H. Li, H. Li, W. Wang, Y. Tao, S. Wang, Q. Yang, Y. Jiang, C. Zheng, W. Huang, R. Chen, *Angew. Chem. Int. Ed.* **2020**, *59*, 4756; b) M. Louis, R. Sethy, J. Kumar, S. Katao, R. Guillot, T. Nakashima, C. Allain, T. Kawai, R. Métivier, *Chem. Sci.* **2019**, *10*, 843.

[10] a) S. Ito, *Chem. Lett.* **2021**, *50*, 649; b) M. Kato, H. Ito, M. Hasegawa, K. Ishii, *Chem. - Eur. J.* **2019**, *25*, 5105; c) X. Huang, L. Qian, Y. Zhou, M. Liu, Y. Cheng, H. Wu, *J. Mater. Chem. C* **2018**, *6*, 5075; d) Y. Sagara, S. Yamane, M. Mitani, C. Weder, T. Kato, *Adv. Mater.* **2016**, *28*, 1073.

[11] a) S. Ito, S. Nagai, T. Ubukata, T. Ueno, H. Uekusa, *Cryst. Growth Des.* **2020**, *20*, 4443; b) S. Takahashi, S. Nagai, M. Asami, S. Ito, *Mater. Adv.* **2020**, *1*, 708; c) S. Nagai, M. Yamashita, T. Tachikawa, T. Ubukata, M. Asami, S. Ito, *J. Mater. Chem. C* **2019**, *7*, 4988.

[12] For the MCL properties of chiral luminophores, see: a) K. K. Kartha, V. S. Nair, V. K. Praveen, M. Takeuchi, A. Ajayaghosh, *J. Mater. Chem. C.* **2019**, *7*, 1292; b) R. Yamano, Y. Shibata, F. Kishimoto, S. Tsubaki, Y. Wada, K. Tanaka, *Chem. Lett.* **2018**, *47*, 1228; c) P. Xue, J. Ding, Y. Shen, H. Gao, J. Zhao, *Dyes Pigm.* **2017**, *145*, 12; d) H. Wu, Y. Zhou, L. Yin, C. Hang, X. Li, H. Ågren, T. Yi, Q. Zhang, L. Zhu, *J. Am. Chem. Soc.* **2017**, *139*, 785; e) X. Zhang, L. Zhu, X. Wang, Z. Shi, Q. Lin, *Inorg. Chim. Acta* **2016**, *442*, 56; f) M. Jin, T. Seki, H. Ito, *Chem. Commun.* **2016**, *52*, 8083.

[13] S. Ito, K. Ikeda, S. Nakanishi, Y. Imai, M. Asami, *Chem. Commun.* **2017**, *53*, 6323.

[14] a) W. Shang, X. Zhu, T. Liang, C. Du, L. Hu, T. Li, M. Liu, *Angew. Chem. Int. Ed.* **2020**, *132*, 12911; b) Y. Qi, W. Liu, Y. Wang, L. Ma, Y. Yu, Y. Zhang, L. Ren, *New J. Chem.* **2018**, *42*, 11373; c) S. Ito, T. Yamada, M. Asami, *ChemPlusChem* **2016**, *81*, 1272.

[15] a) S. Ito, K. Ikeda, M. Asami, *Chem. Lett.* **2016**, *45*, 1379; b) M. Asami, A. Hasome, N. Yachi, N. Hosoda, Y. Yamaguchi, S. Ito, *Tetrahedron: Asymmetry* **2016**, *27*, 322.

[16] a) R. Prasad, S. V. Dalvi, *Chem. Eng. Sci.* **2020**, *226*, 115911; b) H. N. Kim, K. S. Suslick, *Crystals* **2018**, *8*, 280; c) J. R. G. Sander, B. W. Zeiger, K. S. Suslick, *Ultrason. Sonochem.* **2014**, *21*, 1908; d) M. D. Luque de Castro, F. Priego-Capote, *Ultrason. Sonochem.* **2007**, *14*, 717; e) G. Ruecoft, D. Hipkiss, T. Ly, N. Maxted, P. W. Cains, *Org. Process Res. Dev.* **2005**, *9*, 923.

[17] As-prepared (*R*,*R*)-**1A** did not crystallize upon heating or exposure to solvents.

[18] For a selected review, see: R. Chandrasekar, *Phys. Chem. Chem. Phys.* **2014**, *16*, 7173.

[19] For relatively small particles, photoluminescence was observed over a wide area of the particle surface (Figure S2b).

[20] a) S. Ito, G. Katada, T. Taguchi, I. Kawamura, T. Ubukata, M. Asami, *CrystEngComm* **2019**, *21*, 53; b) A. Inoue, K. Yoshihara, T. Kasuya, S. Nagakura, *Bull. Chem. Soc. Jpn.* **1972**, *45*, 720.

[21] J. B. Birks, A. A. Kazzaz, T. A. King, *Proc. R. Soc. A* **1966**, *291*, 556.
[22] V. Kumar, B. Sk, S. Kundu, A. Patra, *J. Mater. Chem. C* **2018**, *6*, 12086.
[23] R. D. Pensack, R. J. Ashmore, A. L. Paoletta, G. D. Scholes, *J. Phys. Chem. C* **2018**, *122*, 21004.
[24] The intensity of the presented CPL spectra (Figure 6) is normalized. The weak CPL from **1C** is reflected as the relatively noisy appearance of the CPL spectra of **1C** compared with **1A**.
[25] Although the enantiomeric CPL bands and fluorescence spectra of (*R*,*R*)- and (*S*,*S*)-**1** deviate slightly from the mirror images of one another, this deviation should be attributed to the experimental error of fluorescence spectra caused by the different degrees of crystallinity due to sample preparation (Figure 5).
[26] I_L and I_R denote the intensities of the left- and right-handed CPL observed upon excitation with unpolarized light.
[27] The CPL spectra of **1** in toluene were reported in the Supplementary Information of the previous report (ref. 13).
[28] Another possibility is that the decrease in the g_{CPL} value of **1A** is caused by the waveguide phenomenon.
[29] Y. Kondo, S. Suzuki, M. Watanabe, A. Kaneta, P. Albertini, K. Nagamori, *Front. Chem.* **2020**, *8*, 527.

Entry for the Table of Contents

Insert graphic for Table of Contents here.

Insert text for Table of Contents here.

The solid-state emission of a chiral diamine-linked bispyrene can be switched by applying two different types of mechanical stimuli: Ultrasonication and grinding. Remarkably, the switching of solid-state circularly polarized luminescence has been achieved between the crystalline and amorphous states that can respond to the different mechanical stimuli.

Institute and/or researcher Twitter usernames: